# Electrojet estimates from mesospheric magnetic field measurements

**=list all authors here=**

$^{=number=}$=Affiliation Address=

**Key Points:**

- enter point 1 here
- enter point 2 here
- enter point 3 here

Corresponding author: =name=, `=email address=`

## Abstract

Suggested EGU abstract:

The auroral electrojet is traditionally measured remotely with magnetometers on ground or in low Earth orbit. The long distance, more than 100 km, means that smaller scale sizes are not detected. Because of this, the spatiotemporal characteristics of the electrojet are not known. Recent advances in measurement technology give hope of remote detections of the magnetic field in the mesosphere, very close to the electrojet. We present a prediction of the magnitude of these disturbances, inferred from the spatiotemporal characteristics of magnetic field-aligned currents. We also discuss how a constellation of small satellites carrying the Microwave Electrojet Magnetogram (MEM) instrument (Yee et al., 2020), could be used to essentially image the equivalent current at unprecedented spatial resolution.


## Plain Language Summary

[ enter your Plain Language Summary here or delete this section]

## 1 Introduction

Electrojet traditionally measured from ground + later satellites. Disadvantage: Distance $>$ 100 km, which removes fine scale structures. $\Rightarrow$ electrojet spatial structure is not known

New techniques available (EZIE (?, ?)+ maybe sodium laser measurements (Kane et al., 2018) ), which offer the potential to distinguish between different fine-scale structures in the electrojet.

### 1.1 Prediction of mesospheric magnetic field disturbance magnitudes

Since the mesosphere is resistive and presumably free of electric current, it is expected that magnetic field disturbances there are sensitive to the same part of the ionospheric electric current system as is observed from ground. In polar regions, where the main magnetic field is nearly vertical, this is primarily the divergence-free part of the horizontal ionospheric current (Fukushima, 1976; Untiedt & Baumjohann, 1993; Laundal et al., 2015), since the contributions from field-aligned currents and their curl-free horizontal closure currents cancel.

The current associated with magnetic field perturbations below the ionosphere are often modeled as a so-called equivalent current (Kamide et al., 1981), an electric sheet current density on a spherical shell at some fixed altitude, which can account for the observed magnetic field. In this paper, we use the term electrojet synonymously with the equivalent current. The variation in magnetic field strength as function of distance from the electrojet depends on scale size; large-scale currents are seen at greater distances than small-scale currents. Mesospheric magnetic field measurements will therefore enable us to resolve smaller spatial scales than ground measurements. The purpose of this section is to quantify the height variation of the magnetic field disturbances, based on what we already know about the spatial structure of ionospheric currents.

The key assumption that we use is that the spatial power spectrum of the electrojet is proportional with the spatial power spectrum of the field-aligned electric currents. In contrast to the electrojet power spectrum, empirical estimates of the FAC spatial power spectrum are available. Figure 1A shows the spatial power spectrum of the magnetic field associated with FACs, in bold black, from (Gjerloev et al., 2011), who used satellite magnetometers on the three ST-5 satellites, which flew in a pearl-on-a-string configuration in polar low Earth orbit. Since this orbit intersects the FACs, the determination of small

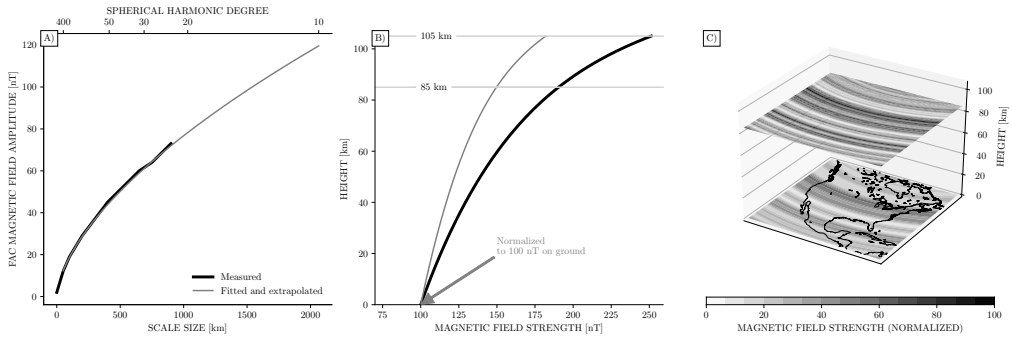


**Figure 1.** B) Altitude variation of $\Delta B$, assuming spatial structure of electrojet is similar to field-aligned currents. Normalized to 100 nT on ground. C)Contour plots of magnetic field of a random electrojet with similar spatial structure (spatial power spectrum) as FACs, shown at 85 km and on ground.

spatial scales is not restricted by distance, as for the electrojet. This particular spatial power spectrum is valid for nightside during disturbed conditions (AL index $< -100$ nT). The spectrum is close to linear on a log-log scale, and we use this property to extrapolate to scale sizes which are longer than those considered by (Gjerloev et al., 2011). The fitted and extrapolated curve is shown in gray.

The curves in Figure 1A, which represents the average magnitude of FAC magnetic field disturbances as function of scale size, is now assumed to also describe the spatial scale of the electrojet at zero distance from the current sheet. With this assumption, we can derive the radial variation of the magnetic field using results from spherical harmonic analysis. Equation 118 of (Sabaka et al., 2010) describes the squared magnetic field, averaged over a sphere at radius $r \leq R$, where $R$ is the current sheet radius, as follows

$$\langle \mathbf{B}(r)^2 \rangle = \sum_{n=1}^{\infty} n \left(\frac{r}{a}\right)^{2n-2} \sum_{m=0}^{n} [(q_n^m)^2 + (s_n^m)^2] = \sum_{n=1}^{\infty} n \left(\frac{r}{a}\right)^{2n-2} A_n. \quad (1)$$

$n$ and $m$ are spherical harmonic degree and order, respectively; $a = 6371.2$ km is a reference radius; and $q_n^m$ and $s_n^m$ are spherical harmonic coefficients. On the right hand side, the sum over spherical harmonic order $m$ is written as $A_n$. The terms in the sum represent the extent to which each degree $n$ contributes to the squared magnitude of the magnetic field.

We assume that the curves in Figure 1A represent the square root of this quantity, at $r = R$. The scale size $L$ and spherical harmonic degree $n$ are related by $\pi R_{FAC}/L$, where $R_{FAC}$ is the radius at which the power spectrum of Figure 1A was evaluated by (Gjerloev et al., 2011). They mapped their measurements to 200 km altitude. This allows us to solve for $A_n$, and thus calculate the squared magnetic field magnitude, averaged over the sphere, as function of radius $r$ using equation (1). The result is shown in Figure 1B. The thick black line is based only on the part of the spatial power spectrum that (Gjerloev et al., 2011) measured, and the grey line is based on an extrapolation to include scale sizes up to spherical harmonic degree $n = 10$. It is clear that when larger scale sizes are included, the radial variation is less dramatic. The current sheet layer was placed at 105 km. Both curves are normalized such that the magnetic field perturbation on ground is 100 nT. The two curves show about 50% and 90% increases from ground to 85 km.

Figure 1C shows contour plots of the magnetic field magnitude at 0 km and at 85 km, for an equivalent current whose magnetic field has the same power spectrum as used with

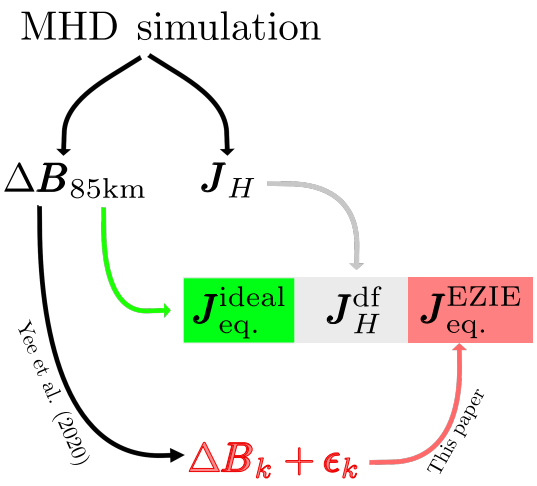


**Figure 2.** PRELIMINARY FIGURE: Schematic to illustrate what is done in this paper: Calculate equivalent current based on realistic measurements from EZIE, and compare the result to 1) equivalent current calculated from an ideal distribution of perfect measurements of $\Delta \boldsymbol{B}$ at 85 km, and 2) the divergence-free part of the horizontal ionospheric currents.

the grey line in Figure 1B. This is done by assigning random spherical harmonic coefficients $q_n^0$ and $s_n^0$ which obey $(q_n^0)^2 + (s_n^0)^2 = A_n$. Longitudinal variations ($m > 0$) are ignored. The figure is not meant to show a realistic magnetic field, but rather to visualize the difference in spatial structure in the magnetic field disturbances at ground and in the mesosphere.

## 2 Resolving electrojet using mesospheric magnetic field measurements

Point: Demonstrate / quantify increased capability in determining electrojet structure with meospheric measurements compared to ground

Subsections:

1. EZIE mission concept
2. MHD simulation details
3. Electrojet inversion

### 2.1 EZIE mission concept

Description of mission: Grid, time resolution, precision (basically going from spectrum to B + error)

Limitations of look direction

### 2.2 Test simulation

Description and plots of MHD simulation and snapshot(s) that we will use.

Description of the simulated data: How is the (perfect) MHD output used to produce measurements on grid with noise / uncertainty etc. Much of this is covered in (Yee et al., 2020)

Description of ideal figures ($\boldsymbol{J}_{eq}^{ideal}$ and $\boldsymbol{J}_{H}^{df}$): $\boldsymbol{J}_{eq}^{ideal}$ is the equivalent curent at 110 (?) km altitude calculated with perfect knowledge about the magnetic field at 85 km. This is what we would get if we had no noise, and perfect spatial coverage. $\boldsymbol{J}_{H}^{df}$ is the divergence-free part of the horizontal current. $\boldsymbol{J}_{eq}^{ideal}$ and $\boldsymbol{J}_{H}^{df}$ are expected to be very similar, but not exactly: $\boldsymbol{J}_{eq}^{ideal}$ does not have spatial structures < distance to electrojet, and it has contributions from magnetospheric currents. $\boldsymbol{J}_{H}^{df}$ has all spatial scales of the MHD simulation, and no contribution from magnetosphere.

### 2.3 Electrojet inversion

Description of algorithm - this is the main section of the paper describing the details of the inversion. Rough description:

- Input: Magnetic field at 85 km on a grid - defined by satellite orbit, 4 viewing directions, and sampling frequency/integration time. Three magnetic field components with different errors every direction - and correlated errors so we can not use least squares techniques directly
- Technique: Place divergence-free spherical elementary current systems (SECS) (Amm, 1997; Vanhamaki & Juusola, 2020) on a grid (details tbd) and find the amplitudes that fit the measurements. Several MHD model snapshots should be used to find an optimal grid + regularization parameters.
- With known divergence-free SECS amplitudes, plot the divergence free current and compare to the ideal currents discussed above

## 3 Discussion

Summary and discussion of assumptions and implications. Below are some suggested sections about the limitations in the approach of this paper.

### 3.1 Effect of weighted volume emission

Can we merge/combine the inversions: Instead of spectrum → magnetic field → equivalent current, we do spectrum → equivalent current.

use probabilistic inversion methods?

### 3.2 Effect of uncertainties in measurement location

There is an uncertainty in the location of the measurements (where the emission comes from). What is the corresponding uncertainty in electrojet estimate? This probably requires different inversion methods. (related to previous subsection... )

### 3.3 Effect of temporal variations

In this paper we work with snapshots of MHD model. What are the effects of time variations?

**Acknowledgments**
Enter acknowledgments, including your data availability statement, here.

## References

Amm, O. (1997). Ionospheric elementary current systems in spherical coordinates and their application. *J. Geomag. Geoelectr.*, 947-955.

Fukushima, N. (1976). Generalized theorem for no ground magnetic effect of vertical currents connected with pedersen currents in the uniform-conductivity ionosphere. *Rep. Ionos.Space Res.Jap*, *30*, 35-50.

Gjerloev, J. W., Ohtani, S., Iijima, T., Anderson, B., Slavin, J., & Le, G. (2011). Characteristics of the terrestrial field-aligned current system. *Annales Geophysicae*, *29*(10), 1713–1729. doi: 10.5194/angeo-29-1713-2011

Kamide, Y., Richmond, A. D., & Matsushita, S. (1981). Estimation of ionospheric electric fields, ionospheric currents, and field-aligned currents from ground magnetic records. *J. Geophys. Res.*, *86*, 801-813. doi: 10.1029/JA086iA02p00801

Kane, T. J., Hillman, P. D., Denman, C. A., Hart, M., Phillip Scott, R., Purucker, M. E., & Potashnik, S. J. (2018). Laser remote magnetometry using mesospheric sodium. *Journal of Geophysical Research: Space Physics*, *123*(8), 6171-6188. doi: 10.1029/2018JA025178

Laundal, K. M., Haaland, S. E., Lehtinen, N., Gjerloev, J. W., Ostgaard, N., Tenfjord, P., ... Anderson, B. J. (2015). Birkeland current effects on high-latitude ground magnetic field perturbations. *Geophys. Res. Lett.*. doi: 10.1002/2015GL065776

Sabaka, T. J., Hulot, G., & Olsen, N. (2010). Handbook of geomathematics. In W. Freeden, M. Z. Nashed, & T. Sonar (Eds.), (pp. 503–538). Berlin, Heidelberg: Springer Berlin Heidelberg. doi: 10.1007/978-3-642-01546-5_17

Untiedt, J., & Baumjohann, W. (1993). Studies of polar current systems using the IMS Scandinavian magnetometer array. *Space Sci. Rev.*, 245-390.

Vanhamaki, H., & Juusola, L. (2020). Introduction to spherical elementary current systems. In *Ionospheric multi-spacecraft analysis tools* (pp. 5–33). ISSI Scientific Report Series 17. doi: 10.1007/978-3-030-26732-2_2

Yee, J. H., Gjerloev, J. W., & Wu, D. L. (2020). Remote Sensing of Magnetic Fields Induced by Electrojets From Space: Measurement Techniques and Sensor Design. *jgr?*.